Hydrological Controls on Methylmercury Distribution and Flux in a Tidal Marsh

Hua Zhang, Kevan B. Moffett, Lisamarie Windham-Myers, Steven M. Gorelick

Supporting Information

Content

Location of domain boundary

The southeastern boundary of the domain was modeled as a no flow/symmetry boundary. It was placed along a subtle height of land dividing the study area marsh from the adjacent marsh, roughly equidistant between the study area channel and the next channel over. This choice was made because there was greater confidence this line should act as a groundwater divide. Also, this choice enabled simulation of bank storage/exfiltration into both banks of the southern channel, thereby properly completing the water balance of the site. This boundary was not at the centerline of the channel for three reasons:

(1) Groundwater discharge to the tidal channel was one of the quantities of interest and treating the channel centerline as the boundary would have eliminated half the possible flux making volumetric relations of simulated seepage volumes to measured channel solute concentrations (which naturally resulted from interaction with both banks) much more uncertain.

(2) It was not clear that the channel centerline should in fact be a symmetry boundary[1]. With oscillating flow directions and large water bodies to both the north and east, we preferred to take the height of land to the south of the channel as a more certain groundwater and surface water divide and therefore permit asymmetric seepage to either bank of that southern channel if it should be appropriate. As shown on the aerial image in Figure 1, some small channels seem to cross the south-eastern boundary. However, field observation showed that those channels were small, almost hidden hanging channel (see photo below on the left) and in fact high-up on the main channel bank (see photo below on the right) like ‘hanging valleys’. For the sake of defining any kind of reasonably sized boundary around the site, it was judged that the volumetric error associated with ‘cutting off’ this small side channel was likely not more than few percent over the whole model domain – well within the overall uncertainty of the whole model.

(3) Even if those very small side channels participate in some exchange with the adjacent marsh, the physics of tidal flooding of the next marsh to the south requires that somewhere within this very small side channel there occurs a stagnation point where the flood water flows from each marsh balance (and ebb flows, during ebb tide). Our choice of model boundary therefore can essentially be interpreted as assuming that a stagnation point occurs close to the main channel; the error associated with this choice is therefore not so much one of a possible large amount of

missing flow, but of a small amount of additional storage in that channel if the true stagnation point is further to the southeast.

(a) A small, hidden hanging channel

(b) A major channel

Photos were taken by K.B. Moffett.

(1) Moffett, K. B.; Gorelick, S. M.; McLaren, R. G.; Sudicky, E. A., Salt marsh ecohydrological zonation due to heterogeneous vegetation-groundwater-surface water interactions. *Water Resour. Res.* **2012,** *48, W02516*, DOI: 10.1029/2011wr010874.

Boundary and initial conditions of hydrological simulation

No horizontal flow was permitted across the landward marsh edge boundaries (left and bottom of model domain shown in Figure 1), nor vertical groundwater flow across the model base at 10 m depth below sea level. The model employed spatially-variable sediment hydraulic conductivity (from 7×10^{-2} to 7×10^{-4} m day^{-1}, with clay sediment unsaturated hydraulic characteristic curves[1,2]) and surface boundary conditions (evapotranspiration rates) based on vegetation patterns derived from field measurements and distributed linearly through vegetation zone-specific rooting depths. [3] Initial conditions were hydraulic heads resulting from 7 days of simulated gravity drainage starting with a fully saturated domain.[3] The model was calibrated to data from 28 piezometers in 14 shallow/deep pairs from December 2007,[3] and was then driven by the tidal conditions from the two days of fieldwork in this study (i.e., January 26 and September 26, 2011).

References

(1) Schaap, M. G.; Leij, F. J., Improved prediction of unsaturated hydraulic conductivity with the Mualem-van Genuchten model. *Soil Sci. Soc. Am. J.* **2000,** *64* (3), 843-851.

(2) van Genuchten, M. T., A closed-form equation for predicting the hydraulic conductivity of unsaturated soils. *Soil Sci. Soc. Am. J.* **1980,** *44* (5), 892-898.

(3) Moffett, K. B.; Gorelick, S. M.; McLaren, R. G.; Sudicky, E. A., Salt marsh ecohydrological zonation due to heterogeneous vegetation-groundwater-surface water interactions. *Water Resour. Res.* **2012,** *48, W02516*, DOI: 10.1029/2011wr010874.

Sampling during low tide and quality control of geochemical analysis

The bottle was held in a small depression in the streambed without disturbing the sediment and allowed to fill to overflowing. Pore water was sampled under tension using field conditioned stainless-steel sippers and polyethylene syringes in January at nine locations at depths of 8, 20, 32 and 44 cm and in September at eight locations at the depth of 26 cm (Figure 1).

The matrix spike recovery was 93% +\- 9% (n=5). At least 10 percent of all MeHg analyses were run in replicate and agreed within ±20 percent (acceptance criteria for the batches run). Daily method detection limit (as run) was 0.004 ng/L for MeHg and 0.02 ng/L for THg. Using a 1" manual corer, a sediment section from 0-14 cm below ground surface was recovered and sealed in a zip-top bag, a second section from 14-28 cm recovered from the same hole into a second bag, and a third section from 28-50 cm in September 2011. Sediment samples were dried, prepared, analyzed for THg and other metals using X-ray fluorescence spectrometry as in Dittmar *et al.*[1]

Reference

(1) Dittmar, J.; Voegelin, A.; Roberts, L. C.; Hug, S. J.; Saha, G. C.; Ali, M. A.; Badruzzaman, A. B. M.; Kretzschmar, R., Spatial distribution and temporal variability of arsenic in irrigated rice fields in Bangladesh. 2. Paddy soil. *Environ. Sci. Technol.* **2007,** *41* (17), 5967-5972, DOI: 10.1021/es0702972.

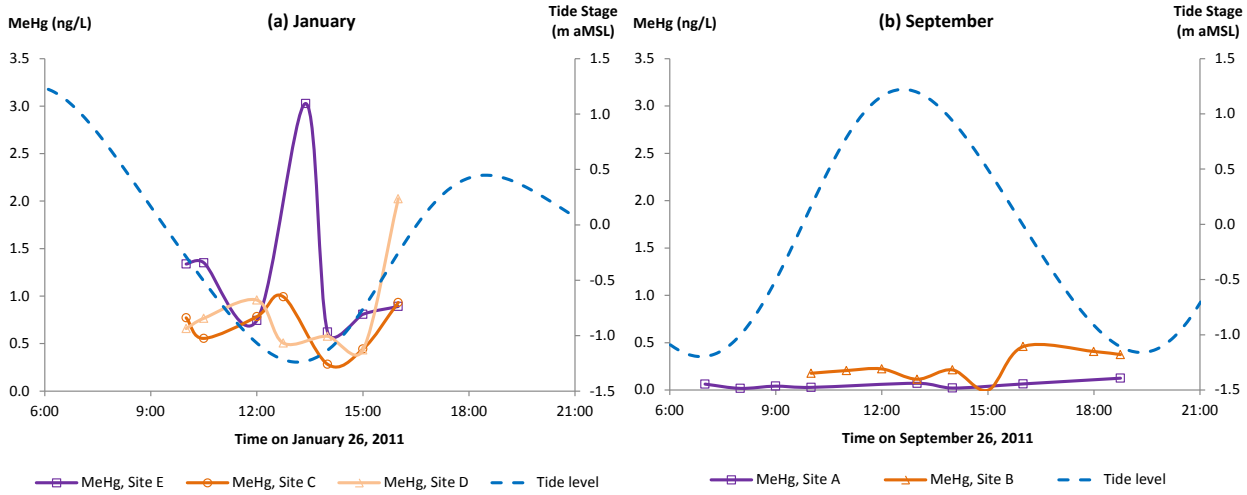

Figure S1. Variation of surface water MeHg concentrations during the tidal cycles. There was no consistent effect of tidal cycle on the temporal variability of MeHg concentrations in surface water. Locations of surface water sampling (A to E) are shown in Figure 1. Detection limit and the Site B measurement on September 26 at 15:00 were 0.004 ng/L. MeHg concentrations at Site A (main channel) in September (Table S1) were used to calculate the MeHg flux between the marsh and the estuary.

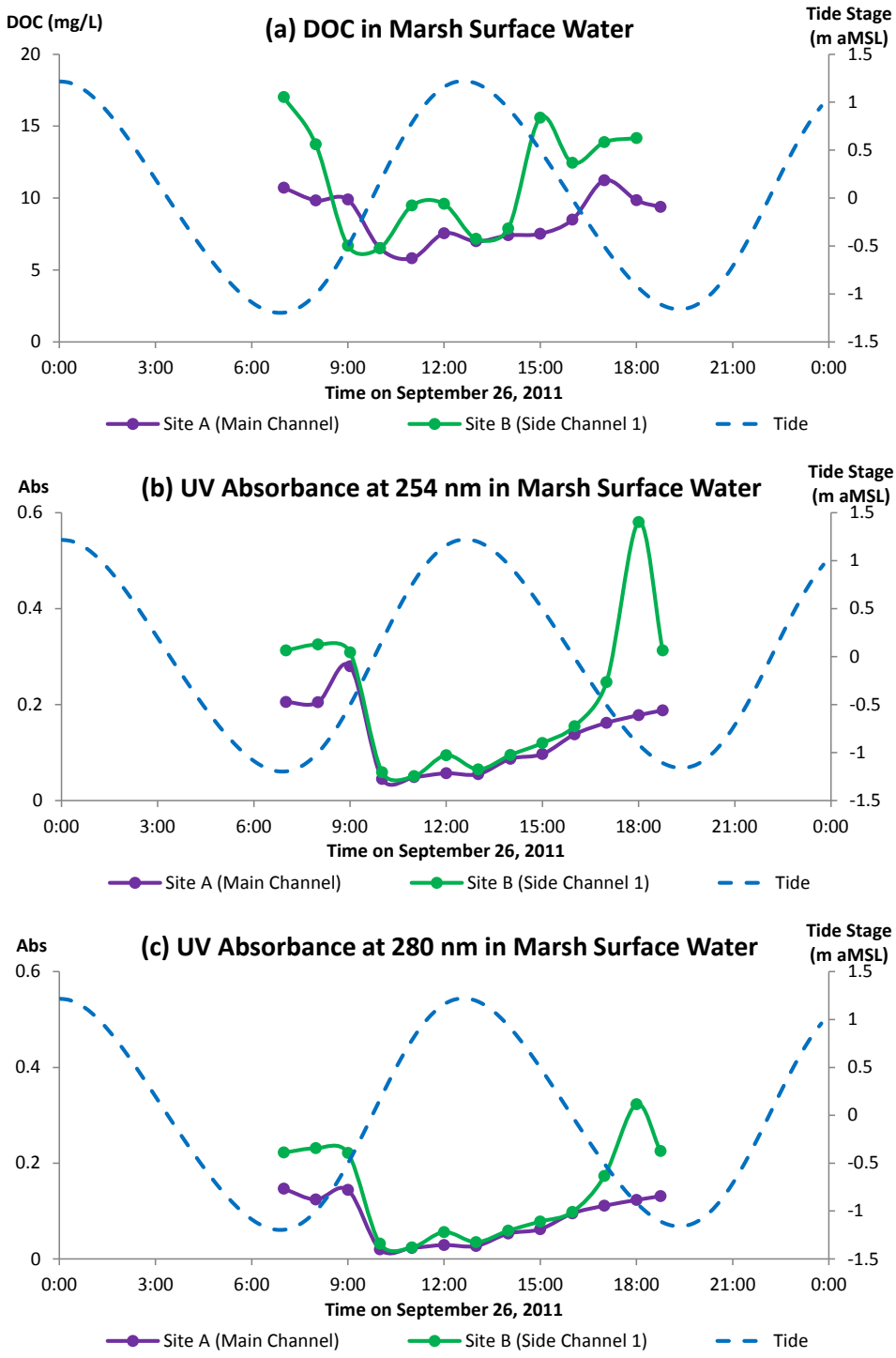

Figure S2. Variation of DOC concentrations and UV absorbance levels (which in ratio deliver specific UV absorbance, SUVA) during the tidal cycle in September 2011. DOC concentrations and SUVA levels showed clear responses to tide levels but were not significantly related to MeHg concentrations in the surface water (as shown in Figure S1).

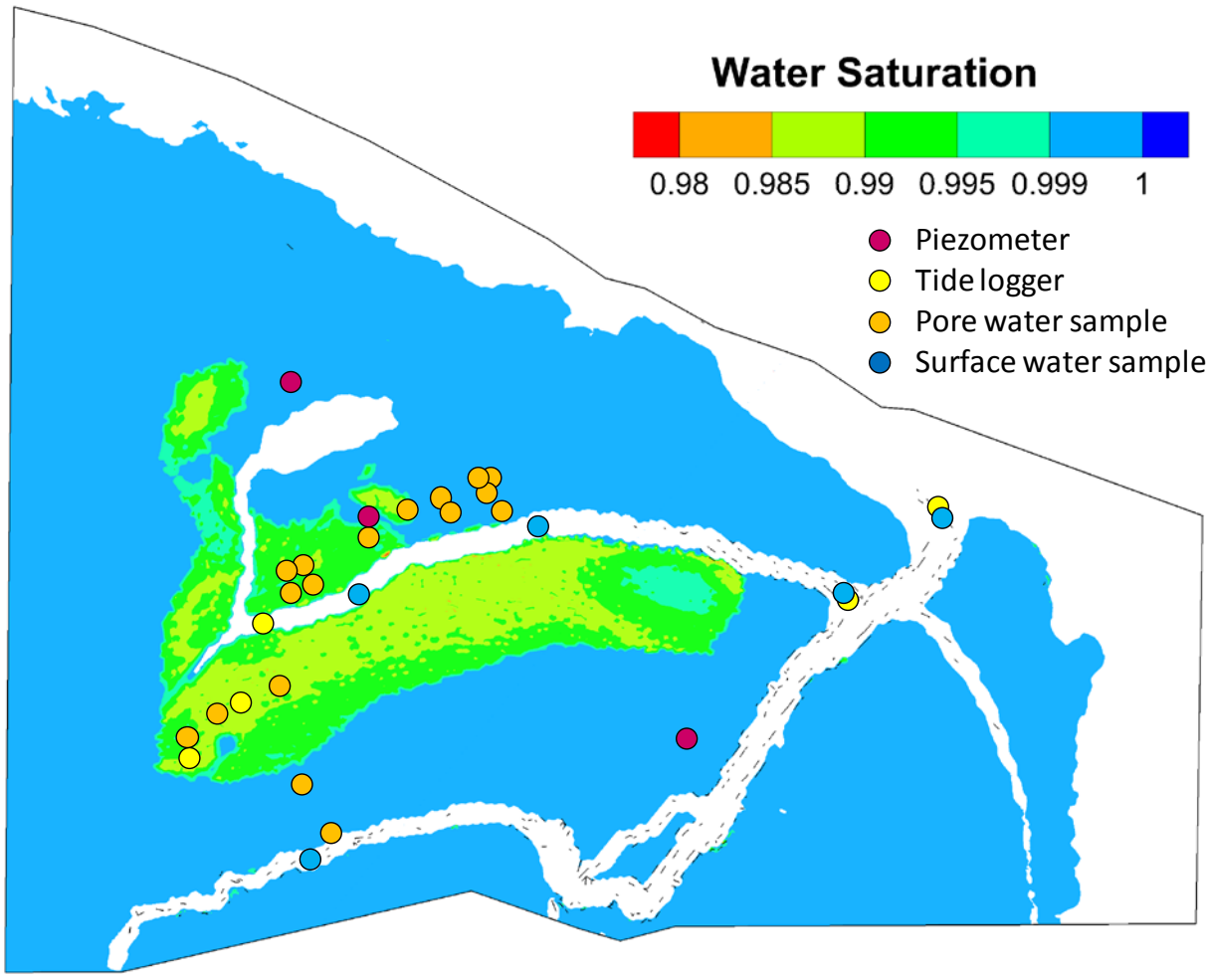

Figure S3. Water saturation conditions at the depth of 10 cm at high tidal flood stage. The aerated zone (green-yellow) was coincident with the region of low hydraulic conductivity sediments in the central marsh that also hosted vegetation with rooting depth greater than 10 cm. Areas where the persistent unsaturated pocket existed accounted for 16% of the total marsh area.

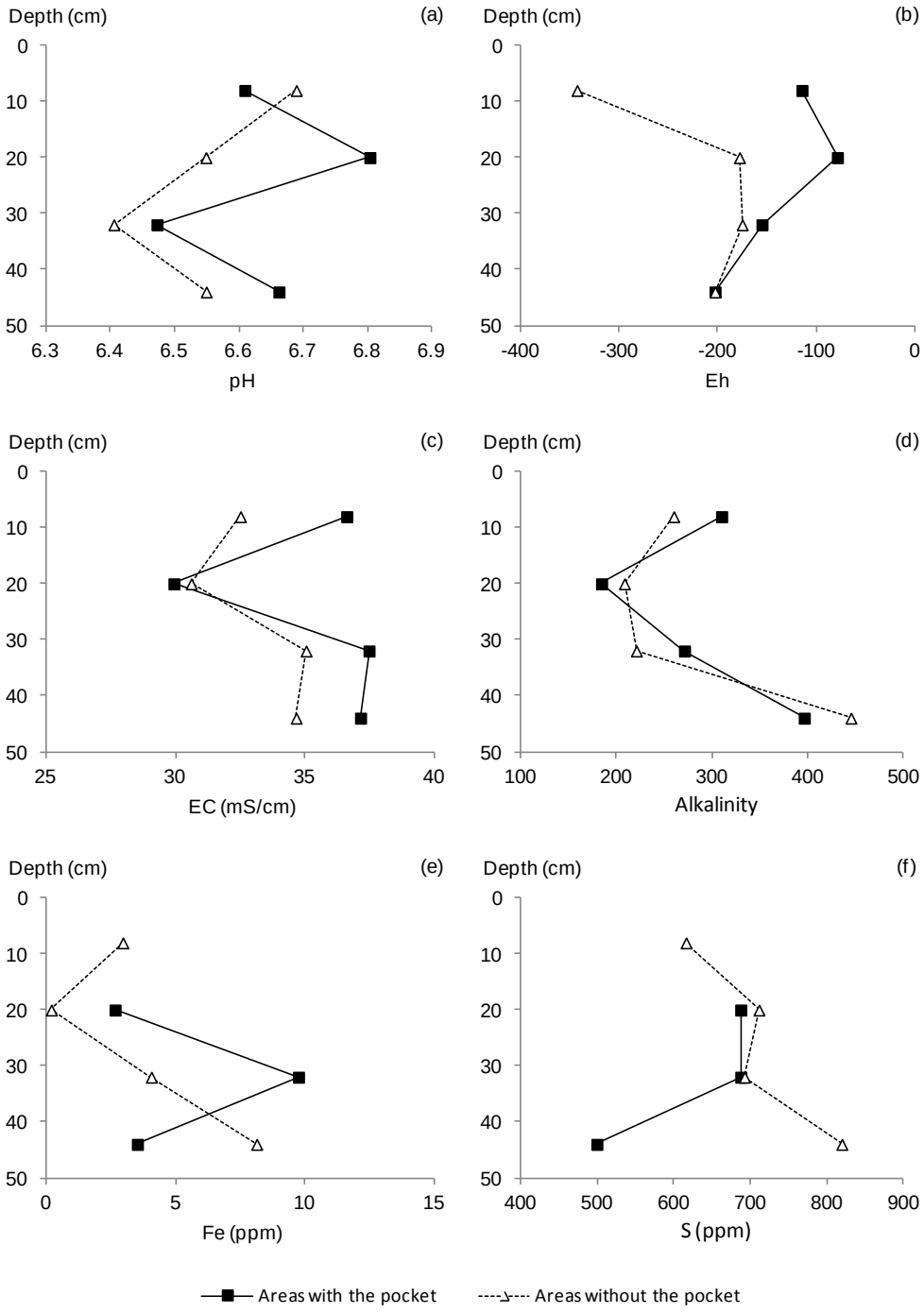

Figure S4. Variations of pore water geochemical parameters with depth (January data), comparing marsh areas hosting a persistently unsaturated pocket in the root zone and those without such a pocket.

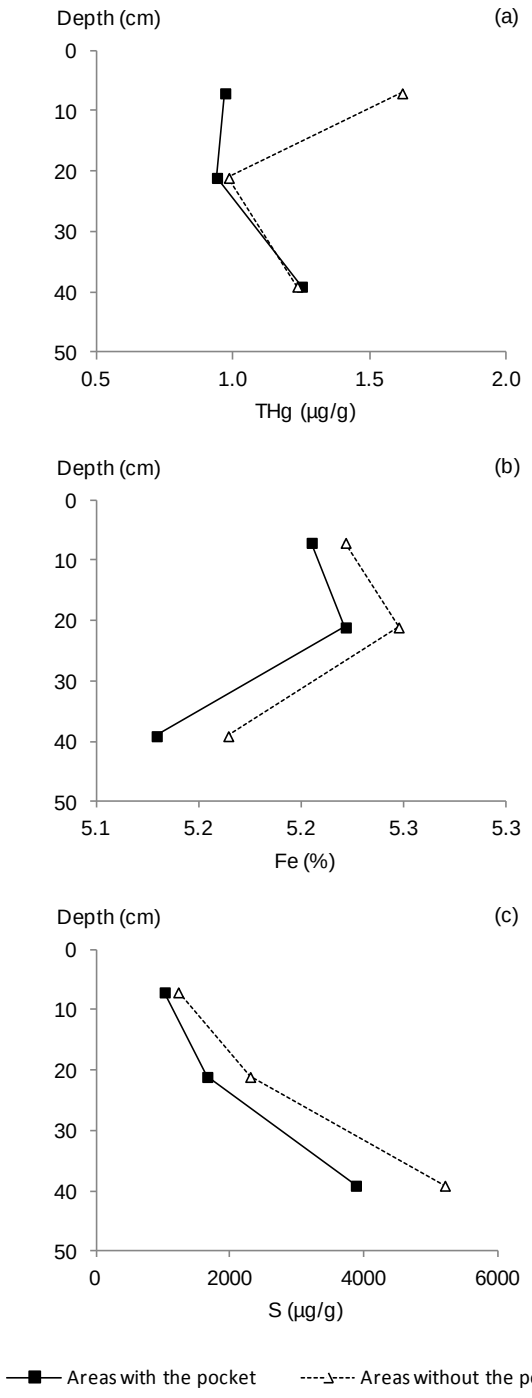

Figure S5. Variations of sediment geochemical parameters with depth (January samples), comparing marsh areas hosting a persistently unsaturated pocket in the root zone and those without such a pocket.

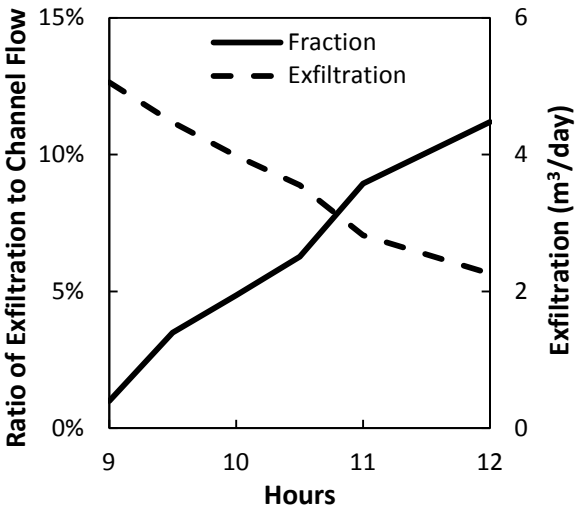

Figure S6. Groundwater exfiltration volume and its contribution to channel discharge during the late stage of ebb tide, summed over the whole marsh.

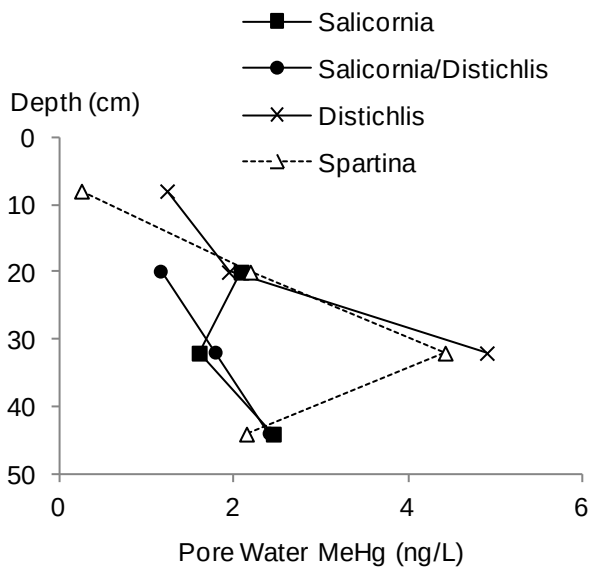

Figure S7. Pore water MeHg concentrations in the root zone of dominant marsh vegetation species.

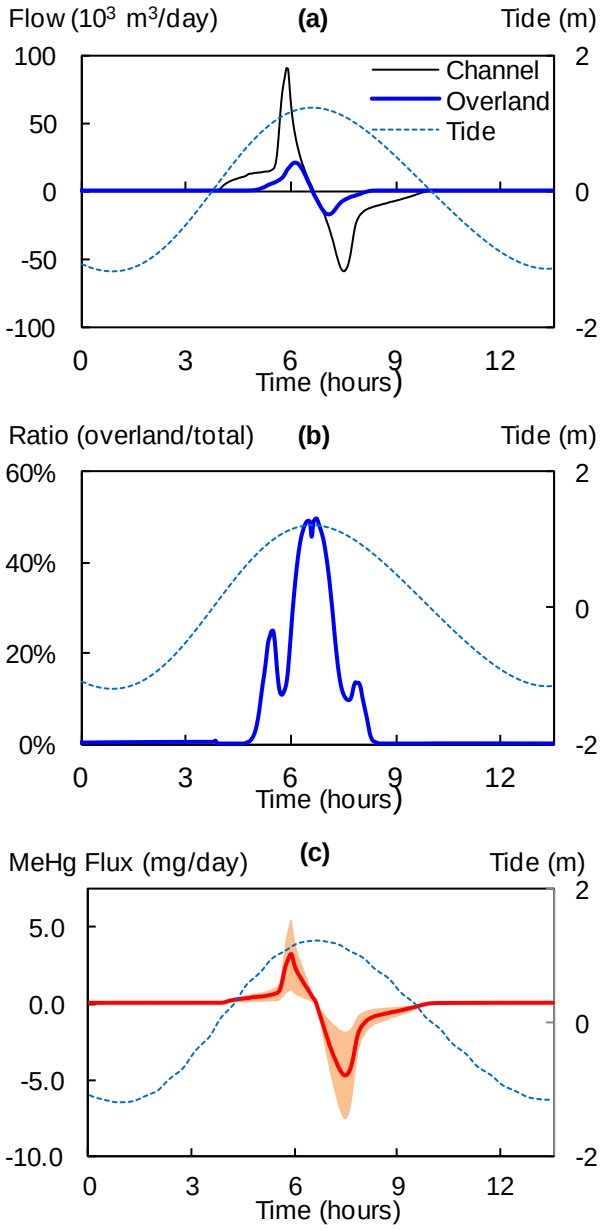

Figure S8. The marsh-estuary exchange of water and MeHg over a tidal cycle in September 2011: (a) the magnitude of overland and channelized flow at the marsh edge/channel mouth, (b) the ratio of overland flow to total flow, and (c) the MeHg flux. In (a) and (c), positive values indicate landward flux and negative values seaward flux. In (c), solid line indicates the average flux and shaded area indicates error bounds; flux is calculated as the product of simulated marsh-wide water fluxes and measured MeHg concentrations in the main channel.

Table S1. Comparison of pore water MeHg concentrations with regard to the occurrence of unsaturated pockets on January 26, 2011 (unit: ng/L).

Depth (cm)	**Areas without the pockets**		**Areas with the pockets**	
	mean	std	mean	std
8	0.25	*-	1.23	*-
20	1.10	1.39	2.45	1.61
32	1.94	1.71	3.26	1.79
44	2.22	0.12	2.39	0.48

* Only one sample was collected at this depth.

Table S2. MeHg and THg concentrations on September 26, 2011.

Location	Time	MeHg(ng/L)	THg (ng/L)	MeHg/THg
Site A	7:00 AM	0.062	-	
(main channel)	8:00 AM	0.017	16.54	0.10%
	9:00 AM	0.041	10.06	0.41%
	10:00 AM	0.028	28.69	0.10%
	11:00 AM	0.004*	1.61	0.25%
	1:00 PM	0.071	19.23	0.37%
	2:00 PM	0.021	25.89	0.08%
	4:00 PM	0.064	-	
	6:45 PM	0.125	16.61	0.75%
Side B	10:00 AM	0.18	8.73	2.03%
(side channel 1)	11:00 AM	0.21	4.10	5.00%
	12:00 PM	0.22	15.44	1.44%
	1:00 PM	0.11	14.49	0.78%
	2:00 PM	0.21	5.32	3.99%
	4:00 PM	0.46	13.11	3.50%
	6:45 PM	0.37	17.42	2.15%
Pore water 1	10:25 AM	0.146	41.99	0.35%
Pore water 2	11:00 AM	0.004	22.68	0.02%
Pore water 3	10:36 AM	0.227	40.24	0.56%
Pore water 4	10:43 AM	0.285	26.16	1.09%
Pore water 5	11:11 AM	0.211	45.07	0.47%
Pore water 6	11:26 AM	0.101	38.45	0.26%

*Below MDL (0.004 ng/L).